

ZIBELINE INTERNATIONAL™
PUBLISHING

ISSN: 2521-0890 (Print)

ISSN: 2521-0491 (Online)

CODEN: GBEEB6



RESEARCH ARTICLE

RETROGRESSION OF ORTHOPYROXENE – BEARING CHARNOCKITIC GNEISS AROUND IKERAM-IBARAM AKOKO, SOUTHWESTERN NIGERIAAnthony Victor Oyeshomo^a, Uwe Altenberger^b, Anthony Bolarinwa^c^a Department of Earth Sciences, Adekunle Ajasin University, Akungba-Akoko, Nigeria^b Institute of Earth and Environmental Science, Universität Potsdam, Germany^c Department of Geology, University of Ibadan, Ibadan, Nigeria*Corresponding author's e-mail: anthony.oyeshomo@aaau.edu.ng

This is an open access journal distributed under the Creative Commons Attribution License CC BY 4.0, which permits unrestricted use, distribution, and reproduction in any medium, provided the original work is properly cited

ARTICLE DETAILS

Article History:

Received 20 March 2024

Revised 10 April 2024

Accepted 30 May 2024

Available online 01 June 2024

ABSTRACT

This paper presents the petrography and mineral chemistry of charnockitic gneisses exposed at Ikeram-Ibaram within the Precambrian Basement Complex of southwestern Nigeria. Quartz, plagioclase, perthite, amphibole, biotite and orthopyroxene are essential minerals, while apatite, ilmenite, magnetite and zircon are accessories. Orthopyroxene is ferro-hypersthene (En₄₄Fs₅₆Wo₀) with low TiO₂, CaO contents, but high in MgO compositions. Orthopyroxene is mantled by hornblende and relicts of biotite grains are found within orthopyroxene as inclusions. Plagioclase is andesine and occur as inclusions in other minerals. Biotite has high concentration of TiO₂, but poor in CaO. Ilmenite and magnetite are closely associated with orthopyroxene. Rare earth element (REE) displays enrichment in light REE and depletion in heavy REE with negative Eu anomaly. Biotite as relicts in orthopyroxene and amphibole mantling orthopyroxene are clear evidences of retrograde metamorphic events. The mineral reactions suggest the retrogression of the charnockitic gneisses that are products of rehydration processes. These relationships between pairs of minerals indicate retrogressive form of metamorphism at the transition from granulite facies to amphibolites facies.

KEYWORDS

ferro – hypersthene, rehydration, retrograde event, rare earth element, granulite.

1. INTRODUCTION

Pyroxene – bearing gneisses are often referred to as charnockitic gneisses, especially when they contain hypersthene. The word “charnockite” was first introduced by Holland to honour Job Charnock (founder of Calcutta, India) whose tombstone was made of the rock (Holland, 1900). He defined charnockite as quartz- feldspar – hypersthene – iron ore rock. Charnockites are orthopyroxene – bearing anhydrous granitoids (Holland, 1900; Le Maitre, 2002). They occur as patches in host gneisses, magmatic and metamorphic in origin, Charnockites are restricted to high grade granulite terrains and in cases associated with rocks of amphibolites facies. They are formed from both igneous and sedimentary protoliths during high grade metamorphism under low activity of water (Rajesh et al., 2012). Parras described an orthopyroxene – garnet bearing dark greenish metamorphic rock of zones of dehydration as “incipient charnockite” similar to the rock observed (Holland, 1900; Parras, 1958).

These rocks were found to occur in many parts of southern India and the world. Pichamuthu opined that original protolith was dehydrated by influx of CO₂ released from underplated basalts or carbonates (Pichamuthu, 1960). Harlov considered influx of external fluid, preferably of low a- H₂O during granulite metamorphism as the main cause of charnockitisation (Harlov, 2012). A group researcher attributed the retrogression of pyroxene bearing gneiss of Iboropa Akoko, southwestern Nigeria to retrograde metamorphic event (Oziegbe et al., 2020). Some researcher also, documented the occurrence of dehydrated charnockite of North China Shield and concluded that they were formed at ultra – high temperature conditions of about 890^o – 970^oC (Yang et al., 2014). In this

research, the study area, Ikeram – Ibaram is underlain by rocks of the southwestern Basement Complex.

The rocks consist of migmatite –gneiss – quartzite complex, with charnockites and granites occurring as enclaves. The migmatitic gneisses of this area are composed of three components, which in most cases occur in same outcrop. These components are the paleosome (early gneiss), leucosome (granite and/ or granite gneiss) and neosome (amphibolites bands). Ikeram – Ibaram is about 9km north of Ikare. The charnockitic gneiss of Ikeram – Ibaram is dark grey and foliated. Rahaman and Ocan worked on the nature of granulite metamorphism of Ikare area, but devoid of micro-chemical data (Rahaman and Ocan, 1988). Therefore, this paper is aimed at presenting the petrography, mineral chemistry as well as bulk rock geochemistry of the charnockitic gneisses as exposed at Ikeram – Ibaram, southwestern Nigeria.

2. LOCATION AND ACCESSIBILITY OF THE STUDY AREA

The study area, Ikeram - Ibaram Akoko is situated in the northernmost part of Ondo State, southwestern Nigeria. It lies within latitudes 7^o 35' – 7^o 38'N and longitudes 5^o 48' – 5^o 55'E (Figure 1). The area is linked up with motorable roads from neighbouring towns like Erusu, Oke Agbe, Akunnu Akoko and Ajowa. There are numerous footpaths which makes traversing easier. The relief is rugged and marked by rocky undulating hills of migmatites, charnockites and other gneissic rocks. The area is well drained by rivers and streams. Drainage pattern is dendritic and controlled by the underlying lithology and geological structures. The climate is of Tropical rain forest characterized by two alternating seasons

Quick Response Code



Access this article online

Website:

www.geologicalbehavior.com

DOI:

10.26480/gbr.02.2024.82.89

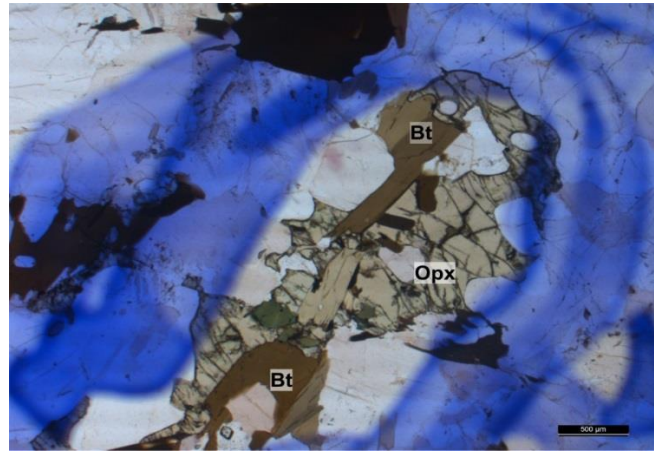


Figure 4: Photomicrograph showing ample evidence of breakdown of biotite to form orthopyroxene in charnockitic gneiss under plane polarized light.

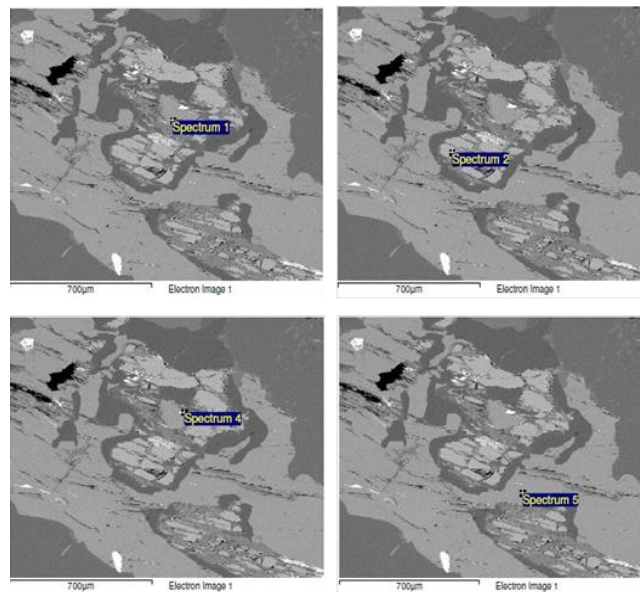


Figure 5: BSE images showing amphibole around orthopyroxene (Spectrum 1), orthopyroxene (Spectrum 2) and magnetite in amphibole (Spectrum 4) and core of amphibole (Spectrum 5) in charnockitic gneiss of Ikeram Akoko.

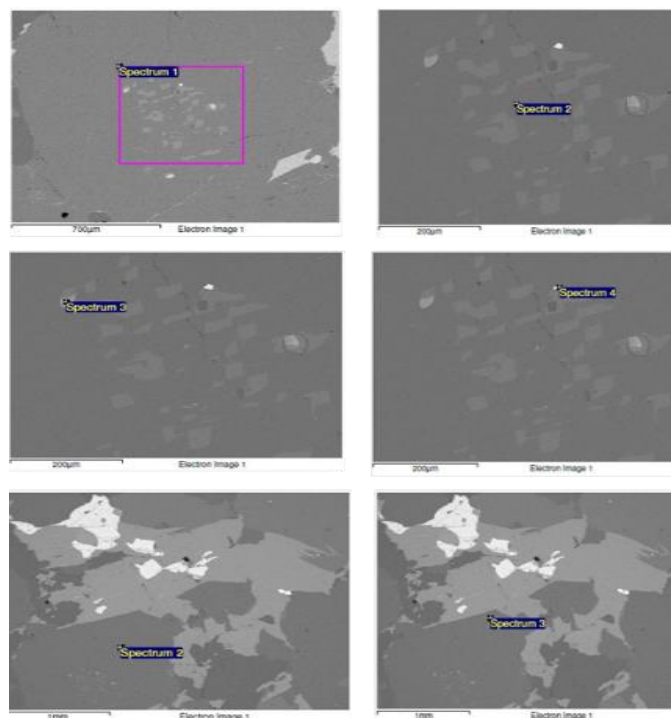


Figure 6: (a) Areal analysis of plagioclase centre with exolutions (Spectrum 1), (b) K-feldspars exolutions in plagioclase (spectrum 2), (c) biotite inclusion in plagioclase (Spectrum 3), (d) magnetite in plagioclase (Spectrum 4), (e) plagioclase (andesine) core (spectrum 2) and plagioclase (andesine) rim (spectrum 3) in charnockitic gneiss around Ikeram Akoko.

Table 1: Representative microprobe data of orthopyroxene in the charnockitic gneiss

Oxides (wt%)	core	rim	core	rim	core	rim	core	rim
SiO ₂	48.96	49.05	49.30	49.90	50.34	50.66	50.45	50.37
TiO ₂	0.06	0.06	0.07	0.05	0.06	0.04	0.07	0.03
Al ₂ O ₃	0.57	0.56	0.60	0.81	0.81	0.68	0.878	0.80
FeO	34.55	34.61	35.19	35.03	30.98	30.38	30.55	30.12
MnO	2.31	2.25	2.18	2.13	1.83	1.78	1.85	1.72
MgO	13.45	13.65	13.18	13.39	15.47	15.65	16.07	15.99
CaO	0.83	1.03	0.79	0.57	0.90	0.65	0.75	0.54
Na ₂ O	0.04	0.05	0.05	0.06	0.04	0.01	0.04	-
K ₂ O	0.01	0.01	-	-	0.01	0.02	0.01	0.03
Sum	100.78	101.27	101.36	101.94	100.44	99.87	100.66	98.88
Structural formula recalculated based on 4 cations and 6 oxygens								
Si	1.91	1.92	1.94	1.96	1.97	1.96	1.95	1.97
Al (iv)	0.03	0.03	0.03	-	-	-	0.04	0.03
Fe ³⁺	0.15	0.14	-	0.08	0.05	0.01	0.06	0.03
Fe ²⁺	0.98	1.00	0.10	1.07	0.97	0.99	0.93	0.96
Mn	0.10	0.10	0.10	0.10	0.06	0.06	0.06	0.06
Mg	0.78	0.80	0.78	0.78	0.90	0.91	0.93	0.93
Ca	0.04	0.04	0.02	0.02	0.04	0.03	0.03	0.02
Moles % End Members								
Wo	0	0	0	0	0	1.00	0	0
En	42.00	43.00	41.00	41.00	47.00	46.00	48.00	48.00
Fs	58.00	57.00	59.00	59.00	53.00	53.00	52.00	52.00

Table 2: Representative microprobe data of hornblende in the charnockitic gneiss

Oxides (wt%)	core	rim	core	rim	core	rim	core	rim	core	rim	core
SiO ₂	41.10	40.79	41.90	41.27	41.57	41.35	40.84	40.53	41.64	41.01	41.31
TiO ₂	1.52	1.09	1.27	1.33	1.45	1.43	1.52	1.08	1.26	1.24	1.27
Al ₂ O ₃	10.89	11.37	10.80	12.20	11.20	11.12	10.74	11.21	10.65	12.03	10.87
FeO	21.60	21.84	21.16	21.63	21.25	21.73	21.60	21.83	21.16	21.62	21.24
MnO	0.56	0.55	0.63	0.54	0.55	0.52	0.55	0.55	0.63	0.54	0.55
MgO	8.17	7.80	8.42	8.00	8.37	8.33	8.02	7.66	8.27	7.85	8.22
CaO	10.91	11.19	11.08	11.42	11.02	11.21	10.95	11.23	11.12	11.46	11.10
Na ₂ O	1.57	1.32	1.52	1.33	1.45	1.43	1.60	1.34	1.54	1.34	1.47
K ₂ O	1.42	1.66	1.31	1.70	1.46	1.50	1.41	1.65	1.30	1.70	1.46
Sum	97.74	97.61	98.09	99.42	98.14	98.62	97.23	97.08	97.57	98.79	97.49
Cations calculated on the basis of 23 oxygens											
Si	6.23	6.21	6.31	6.16	6.25	6.21	6.23	6.22	6.23	6.17	6.25
Al (iv)	1.77	1.79	1.69	1.84	1.75	1.79	1.76	1.78	1.72	1.82	1.75
Al (vi)	0.17	0.25	0.22	0.30	0.21	0.18	0.17	0.24	0.17	0.30	0.19
Ti	0.17	0.13	0.14	0.15	0.16	0.16	0.17	0.12	0.14	0.14	0.14
Fe ³⁺	0.98	0.93	0.92	0.88	0.95	0.98	0.91	0.71	0.89	0.82	0.90
Fe ²⁺	1.76	1.90	1.75	1.82	1.73	1.75	1.84	2.08	1.77	1.90	1.84
Mn	0.10	0.10	0.10	0.10	0.07	0.07	0.10	0.10	0.10	0.10	0.10
Mg	1.85	1.77	1.89	1.78	1.88	1.86	1.82	1.75	1.86	1.76	1.84
Ca	1.77	1.83	1.79	1.83	1.78	1.80	1.79	1.84	1.80	1.84	1.82
Na	0.46	0.39	0.44	0.38	0.42	0.42	0.47	0.54	0.45	0.40	0.42
K	0.27	0.32	0.25	0.32	0.28	0.29	0.27	0.32	0.25	0.32	0.28

4.2.3 Biotite

The micro-chemical composition of biotite is given in Table 3. SiO₂: 35.68 – 36.21%; FeO: 20.72 – 21.93%; MgO: 10.76 – 11.38%; Al₂O₃: 14.55 – 14.93%; TiO₂: 3.60 – 5.21%; CaO: 0.02 – 0.06 and K₂O: 9.46 – 9.76% for both core and rim compositions. The recalculated formula showed that the biotite is siderophyllite.

4.2.4 Plagioclase feldspar

The chemical composition of plagioclase feldspar is presented in Table 4. SiO₂: 56.80 – 58.57%; Al₂O₃: 25.17 – 27.21%; CaO: 6.91 – 8.50%; Na₂O: 6.55

– 7.40% and K₂O: 0.21 – 0.41% for core and rim compositions. In terms of end members, average composition is given as An₃₅Ab₆₂ and An₃₈Ab₆₀ for core and rim compositions respectively.

4.2.5 Alkali Feldspar

The chemical composition of alkali feldspar in the charnockitic gneiss presented in Table 5. SiO₂: 62.70 – 64.61%; Al₂O₃: 18.44 – 18.95%; K₂O: 14.10 – 14.98%; Na₂O: 1.02 – 1.67% and CaO: 0.02 – 0.04 for core and rim compositions. Average compositional range expressed as Or₈₈Ab₁₂Wo₀ indicate microcline.

Table 3: Representative microprobe data of biotite in the charnockitic gneiss

Oxides (wt%)	core	rim	core	rim	core	rim	core	rim
SiO ₂	35.87	35.93	35.99	36.14	36.21	35.96	35.9	35.68
TiO ₂	4.71	4.73	3.96	4.11	5.21	5.04	4.42	3.6
Al ₂ O ₃	14.56	14.93	14.86	14.55	14.67	14.77	14.73	14.78
FeO	20.9	21.24	21.44	21.27	20.72	20.77	21.93	20.76
MnO	0.19	0.23	0.21	0.21	0.28	0.27	0.22	0.2
MgO	10.94	10.91	11.33	11.1	10.76	10.98	11.11	11.38
CaO	0.04	0.06	-	0.02	0.04	0.04	-	0.06
NaO	0.05	0.08	0.01	0.03	0.08	0.06	0.04	-
K ₂ O	9.46	9.58	9.76	9.73	9.7	9.61	9.71	9.66
Sum	96.72	97.69	97.56	97.16	97.58	97.5	98.06	96.12
Cations on the basis of 4 cations, 6 oxygens								
Si	5.4	5.36	5.38	5.42	5.4	5.37	5.36	5.4
Al (iv)	2.58	2.62	2.61	2.51	2.57	2.6	2.6	2.6
Al (vi)	-	-	-	-	-	-	-	-
Ti	0.53	0.53	0.44	0.46	0.57	0.56	0.5	0.45
Fe ²⁺	2.63	2.65	2.68	2.67	2.58	2.6	2.74	2.62
Mn	0.02	0.03	0.02	0.02	0.03	0.03	0.03	0.02
Mg	2.45	2.42	2.53	2.48	2.4	2.44	2.47	2.56
Ca	-	0.01	-	-	-	-	-	0.01
Na	0.01	0.02	-	0.01	0.02	0.01	0.01	-
K	1.81	1.82	1.86	1.86	1.84	1.83	1.85	1.86
Fe ²⁺ /Fe ²⁺ +Mg	0.51	0.52	0.51	0.51	0.52	0.51	0.52	0.5

Table 4: Representative microprobe data of plagioclase feldspar in charnockitic gneiss

Oxides (wt%)	core	rim	core	rim	core	core	rim	core	rim	core	rim
SiO	58.19	58.57	57.93	57.87	57.88	58.17	57.37	57.37	56.8	57.78	57.25
TiO	-	0.08	0.03	0.01	0.07	-	-	-	-	-	-
Al	25.38	25.68	25.17	25.75	25.66	25.92	27.21	26.4	27.24	26.63	26.72
FeO	0.07	0.53	0.07	0.13	0.07	0.1	0.36	0.05	0.02	0.07	0.11
MgO	-	-	-	-	-	-	-	-	-	-	-
MnO	-	0.01	-	0.02	-	0.1	-	-	-	0.01	0.11
CaO	7.05	7.14	6.91	7.27	7.16	7.36	8.4	7.53	8.5	7.76	7.92
Na	7.08	7.15	7.4	7	7.15	7.08	6.81	7.12	6.55	6.81	6.78
K	0.4	0.21	0.31	0.22	0.29	0.41	0.23	0.41	0.21	0.4	0.35
Sum	98.17	99.3	97.82	98.27	98.28	99.14	100.38	98.88	99.32	99.13	99.24
Structural formula recalculated based on 8 oxygens											
Si	2.68	2.63	2.64	2.63	2.63	2.62	2.56	2.6	2.56	2.6	2.58
Ti	-	-	-	-	-	-	-	-	-	-	-
Al	1.36	1.36	1.35	1.37	1.37	1.38	1.43	1.4	1.44	1.41	1.02
Fe ³⁺	-	-	-	-	-	-	0.01	-	-	-	-
Mn	-	-	-	-	-	-	-	-	-	-	-
Mg	-	-	-	-	-	-	-	-	-	-	-
Ca	0.34	0.34	0.33	0.35	0.35	0.35	0.4	0.36	0.41	0.37	0.38
Na	0.62	0.62	0.65	0.61	0.63	0.62	0.6	0.62	0.57	0.6	0.6
K	0.02	0.01	0.01	0.01	0.01	0.02	0.01	0.02	0.01	0.02	0.02
Moles % End Members											
An	34.7	35.1	33.5	36	35	35.6	40	36	41.3	37.8	38.4
Ab	63	63.6	64.8	62.7	63.3	62	58.7	61.7	57.5	60	59.5
Or	2.3	1.3	1.7	1.3	1.7	2.4	1.3	2.3	1.2	1.2	2.1

Table 5: Representative microprobe data of alkali feldspar in the charnockitic gneiss

Oxides (wt%)	core	rim	core	rim	core	rim	core	rim	core	rim
SiO ₂	62.70	62.72	64.28	64.31	64.61	63.63	63.73	63.58	63.60	64.01
TiO	-	0.01	0.01	0.01	0.04	-	0.01	0.01	0.02	0.02
Al ₂ O ₃	18.70	18.95	18.44	18.68	18.78	18.91	18.86	18.95	18.79	18.81
FeO	0.04	-	0.04	-	0.03	0.02	0.01	-	-	-
MnO	-	-	-	-	0.02	-	-	-	-	-
MgO	-	-	-	-	0.01	-	-	-	-	-
CaO	0.03	0.04	0.03	0.04	0.04	0.03	0.04	0.02	-	-
Na ₂ O	1.43	1.02	1.14	1.04	1.41	1.27	1.67	1.14	1.19	1.15
K ₂ O	14.97	14.98	14.98	14.98	14.48	14.71	14.10	14.97	14.56	14.67
Sum	97.57	97.72	99.06	99.24	99.42	98.57	98.42	98.68	98.16	98.66
Structural formula recalculated based on 8 oxygens										
Si	2.96	2.95	2.99	2.98	2.98	2.97	2.96	2.96	2.97	2.98
Ti	-	-								
Al	1.04	1.05	1.01	1.02	1.02	1.04	1.03	1.04	1.03	1.03
Na	0.10	0.10	0.10	0.09	0.12	0.11	0.15	0.10	0.10	0.10
K	0.90	0.90	0.89	0.88	0.85	0.87	0.87	0.89	0.87	0.87
Moles % End Members										
An	0.2	0.2	0.2	0.2	0.2	0.2	0.2	0.1	-	-
Ab	10.2	9.4	10.4	9.5	12.9	11.6	14.7	10.4	11.1	10.7
Or	89.6	90.4	89.4	90.3	86.9	88.2	85.1	89.5	88.9	89.3

4.3 Major Element Geochemistry

The average composition of the major oxides is presented in Table 6. SiO₂ (62 wt%); TiO₂ (0.45 wt%); Al₂O₃ (14.15 wt%); FeO_t (8.18 wt%); MgO (2.71 wt%); MnO (0.08 wt%); CaO (4.05 wt%); Na₂O (3.07 wt%); K₂O (2.26 wt%), P₂O₅ (0.16 wt%) and LOI (0.78 wt%).

4.4 Trace Elemental Composition

The average composition of the compatible elements such as Zn (71.2 ppm); Cr (96.5 ppm) are shown in Table 6. Immobile transition element

such as Nickel (Ni) has average composition of 38 ppm. For the compatible elements such as Barium (Ba), Strontium (Sr) and Rubidium (Rb) have average compositions of 535 ppm, 371.7ppm and 81.8 ppm respectively.

4.5 Rare Earth Element Geochemistry

All samples showed enrichment in light rare earth elements (LREE) and depletion in the heavy rare earth elements (HREE) with negative europium (Eu) anomaly. Eu/Eu* ranged from 0.44 to 0.89 with an average of 0.61 (Table 6).

Table 6: Major oxides (wt%), trace and rare earth elements (ppm) composition of charnockitic gneiss of Ikeram area

Sample No Oxides (wt%)	1	2	3	4	5	6	7	Average
SiO ₂	67.1	61.5	65.3	66.3	66.1	65.0	64.0	65.0
TiO ₂	0.5	0.6	0.5	0.4	0.7	0.5	0.6	0.45
Al ₂ O ₃	13.40	15.20	13.5	13.1	15.9	14.5	13.50	14.15
FeO	8.08	8.11	7.95	8.73	11.23	5.12	8.08	8.18
MnO	0.08	0.09	0.08	0.10	0.13	0.08	0.06	0.08
MgO	1.94	2.88	2.19	1.30	4.09	3.80	2.80	2.71
CaO	3.34	4.65	2.95	3.51	5.82	4.50	3.63	4.05
Na ₂ O	3.14	3.66	2.75	2.68	3.00	2.65	3.65	3.07
K ₂ O	1.37	1.94	3.45	2.68	1.45	2.58	2.35	2.26
P ₂ O ₅	0.07	0.20	0.13	0.18	0.26	0.17	0.13	0.16
LOI	0.72	0.77	0.85	0.77	0.92	0.72	0.72	0.78
Total	99.73	99.68	99.67	99.70	99.64	99.63	99.68	99.67
Trace Elemets(ppm)								
Ba	448	464	607	656	466	465	645	535
Cr	99	72	81	61	179	64	84	91.4
Ga	16	22	18	17	18	17	16	17.7
Nb	< 10	<10	11	11	< 10	11	<10	5.5
Ni	42	43	42	19	44	42	40	38
Rb	50	69	113	97	78	68	98	81.8
Sr	394	567	253	297	349	394	348	371.7
V	93	108	93	65	142	107	68	96.5
Y	<10	20	18	35	23	18	< 10	23.4

Table 6 (Cont): Major oxides (wt%), trace and rare earth elements (ppm) composition of charnockitic gneiss of Ikeram area

Sample No Oxides (wt%)	1	2	3	4	5	6	7	Average
Zn	72	83	58	62	97	57	70	71.2
Zr	135	180	186	250	134	184	180	178.4
K ₂ O/Na ₂ O	0.43	0.53	1.23	1.00	0.48	0.50	1.00	0.73
K/Rb	227.4	233.4	235	229.3	154.3	228.2	229.2	219.5
Ba/Rb	8.96	6.72	5.37	6.76	5.87	6.83	6.17	6.65
Ba/Sr	1.13	0.81	2.40	2.2	1.33	1.18	1.73	1.54
Sr/Y	ND	28.3	14	8.48	15.1	21.8	ND	17.5
Rb/Sr	1.13	0.12	0.46	0.32	0.22	0.17	0.28	
ASI	1.0	0.90	1.0	1.0	1.0	1.0	1.0	0.78
REE (ppm)								
La	45	38	40	49	80	70	46	46
Ce	78	79	81	97	151	150	96	104.5
Pr	10	8.9	9.4	11	16	15	12	11.7
Nd	39	37	39	43	60	42	38	42.5
Sm	7.5	6.2	7.6	8.3	12	6.5	8.2	8.0
Eu	1.5	1.2	2.2	1.2	1.7	1.3	1.2	1.4
Gd	7.0	4.6	7.1	8.1	10	4.0	4.5	6.4
Tb	1.5	0.66	1.1	1.3	1.6	1.2	1.1	1.2
Dy	6.5	3.4	6.2	7.8	9.9	7.5	6.4	6.8
Ho	2.0	0.63	1.2	1.6	2.0	1.2	0.65	1.3
Er	5.7	1.7	3.6	4.6	5.9	4.5	5.8	4.5
Tm	0.17	0.18	0.51	0.65	0.85	0.18	0.62	0.45
Yb	5.6	1.6	3.6	4.4	5.8	5.5	3.8	4.3
Lu	0.60	0.24	0.59	0.66	0.89	0.47	0.25	0.52
∑REE	210.1	185.3	203.1	238.6	357.6	309.4	224.7	247
La/Yb _N	5.46	16.14	7.54	7.56	9.37	8.64	8.92	9.09
Eu/Eu*	0.62	0.65	0.89	0.44	0.46	0.72	0.54	0.61

4. DISCUSSION

Mineral composition of the orthopyroxene analysed for in the charnockitic gneiss of Ikeram - Ibaram is hypersthene. The mineral is found closely associated with amphibole and plagioclase. Further analysis showed that the pyroxene is rich in iron (Fe) and therefore, can be regarded as Ferro-hypersthene. Orthopyroxene is an important component of charnockitic rocks in granulite facies terrains of the world. The CaO content in the ferro-hypersthene analysed is very low. It ranged from 0.48 to 1.22%. Ca atoms per formula does not exceed 1.0 which only occurs in M2 site (Cameron et al., 1981). Similarly, the alumina (Al₂O₃) content is low (< 1.0%) which is suggestive of low-pressure conditions. These are typical of granulite facies pyroxene composition. Oyawoye (1964) attributed formation of charnockite as a result of transformation of biotite, due to influx of iron-rich juvenile fluid. There are other ways by which orthopyroxene could be formed by mineral reactions.

Hornblende + Quartz Clinopyroxene + Orthopyroxene + Plagioclase + K-Feldspar + H₂O (1)

Biotite + Quartz -----Orthopyroxene + K-Feldspar + H₂O (2)

These reactions are indicative of dehydration process due to low water activity (Perchuk et al., 1993). Mineral assemblage shows two generations of biotite and in case have close association with K-Feldspar (Figure 3). Also, biotite relicts in orthopyroxene grain show such dehydration process in the charnockitic gneiss of Ikeram - Ibaram (Figure 4). Dehydration of high-grade rocks in transition zones of amphibolite facies to granulite facies involve partial melting and in cases fluid solid state transformation (Harlov et al., 2006a; Harlov, 2012; Rigby et al., 2011). Corona texture observed where orthopyroxene (ferro-hypersthene) is mantled by amphibole (hornblende) is an indication of retrograde metamorphic event (Figure 5). This retrogression on the charnockite could be as a result of dehydration processes (Cameron et al., 1981). Retrogression involving breakdown of orthopyroxene is not uncommon in granulite terrains (Lasnier, 1977; Srikantappa et al., 1988). Orthopyroxene replaced by amphibole has been described in the granulite facies charnockitic gneiss

of Iboropa Akoko, southwestern Nigeria (Ozeigbe, 2020). In this study, pyroxene viewed from back scattered electron image (BSE) has numerous cracks which could have aided movement of fluids (Figure 5). Relicts of biotite in orthopyroxene is also an indication of retrogression (Figure 4). Amphibole mantling orthopyroxene could have developed in a process in which orthopyroxene reacts with plagioclase and quartz in presence of water. This can be expressed in this equation;

Orthopyroxene + Plagioclase¹ + Quartz + H₂O = Amphibole + Plagioclase² (1)

Similarly, biotite breakdown to form orthopyroxene can be represented by the equation (2)

Biotite + Quartz = Orthopyroxene + K-Feldspar + H₂O (2)

Equation (2) has been written as if they as if they occur in solid state, but quartz, K-Feldspar and water may occur as components in the melt rather than as solid phases (Frost et al., 2008). The biotite is siderophyllite as presented by the mineral chemistry (Table 3). Hornblende and biotite in charnockites have been found to be product of retrograde metamorphism involving pyroxene granulite facies rocks (Cooray, 1961; Cooray, 1962). Hornblende has higher values of magnesium when compared with those of co-existing orthopyroxene but has relatively higher TiO₂ composition (< 1.0%). Researchers linked this to increase in grade of metamorphism (Raase, 1974; Spear, 1981). TiO₂ content is higher in biotite than those of amphibole and orthopyroxene (average: 4.57 for core composition). Higher TiO₂ in biotite had been attributed to increase in stability field of biotite (Dymek, 1983). MgO compositions in hornblende (7.66 -8.42%) are far less to those of orthopyroxene (13.18 - 16.07%) but a bit close to biotite composition (10.76 - 11.38). Plagioclase is dominant feldspar with average composition given as An₃₅Ab₆₂ indicating andesine. The K-feldspar (microcline - orthoclase) has microperthitic texture which is common in high grade metamorphic terrains due to extreme high temperature (Cayzer, 2002). For the trace element composition, there is enrichment in Ba, Sr, Zr, but depletion in Rb. Rollinson and Tarney opined that Rb depletion in TTGs predates metamorphism of granulite facies

(Rollinson and Tarney, 2005). Ratios of Rb/Sr are low, while Ba/Rb are high for all samples of Ikeram-Ibaram charnockitic gneisses. REE patterns indicate LREE enrichment and HREE depletion with negative europium (Eu) anomaly. La/Yb_N ratios are above 5.0 suggesting evolution of the rocks through magmatic differentiation processes (Feng and Kerich, 1990). REE patterns obtained from study is similar to the works of Ozeigbe on retrogression of orthopyroxene-bearing gneiss of Iboropa Akoko and Olarewaju on charnockitic rocks of Ado-Ekiti area of Ondo State, southwestern Nigeria (Ozeigbe, 2020; Iboropa Akoko and Olarewaju, 1988).

5. CONCLUSION

Based on the petrographic evidences and mineral parageneses suggest a retrograde metamorphic event. Biotite relicts in orthopyroxene grains and mantling of orthopyroxene by amphibole are clear evidences of retrograde mineral reactions due to dehydration processes. Numerous microfractures observed in biotite and orthopyroxene grains could have aided migration of fluids that triggered the alterations seen in them. Trace element and Rare earth element (REE) compositions suggest continental behavior and the charnockitic gneiss of Ikeram-Ibaram could have evolved through magmatic differentiation processes.

ACKNOWLEDGEMENTS

I wish to express my gratitude to apl. Prof. Uwe Altenberger, co-author for the use of JEOL-JSM 6510 microprobe analyzer at the Institute of Earth and Environmental Science, Universität Potsdam, Germany during a six-month research visit funded by Tertiary Education Trust Fund (TETFUND) Nigeria.

REFERENCES

- Cameron, M., Papike, J.J., 1981. Structural and chemical variations in pyroxenes. *American Mineralogist*, 66 (1-2), Pp. 1 – 50.
- Cayzer, N., 1969. *Metamorphic Textures*. Pergamon Press, Oxford, England, Pp. 358.
- Cooray, P.G., 1961. The Geology of the area around Rangala. Ceylon Geological Survey Memoir, 2, Pp. 138.
- Cooray, P.G., 1962. Charnockites and their associated gneisses in Precambrian of Ceylon. *The Quarterly Journal of Geological Survey of London*, 118, pp. 239 – 273.
- Dymek, R.F., 1983. Titanium, aluminium and interlayer cation substitutions in biotite from high grade gneisses, west Greenland. *American Mineralogist*, 68 (9-10), Pp. 880 – 899.
- Feng, R., Kerrich, R., 1990. Geochemistry of fine-grained clastic sediments in the Archean – Abitibi greenstone belt, Canada: implication for provenance and tectonic setting. *Geochimica Cosmochimica Acta*, 54, Pp. 1061 – 1081.
- Frost, B.R., Frost, C.D., 2008. On charnockites. *Gondwana Research*, 13, Pp. 30 – 44.
- Harlov, D.E., 2012. The potential role of fluids during regional granulite facies dehydration in the lower crust. *Geosciences Frontiers*, 3, Pp. 813 – 827.
- Harlov, D.E., Johansson, L., Van Den Kerkhof, A, Förster, H.J., 2006a. The role of advective fluid flow and diffusion during localized solid-state dehydration: Sondrum Stenhuggeriet Halmstad, S.W Sweden. *Journal of Petrology*, 47, Pp. 3 – 33.
- Holland, T.H., 1900. The charnockite series, a group of Archean

hypersthentic rocks in Penninsular India. *Memoir of Geological Survey of India*, 28, Pp. 192 – 249.

- Iloje, N.P., 1976. *A new geography of Nigeria*. Metricated Edition, Longman Press.
- Lasnier, B., 1977. *Persistence d'une serie granulitique au coeur du Massif central francois, Haut – Allier: les termes basiques ultrabasiqes et carbonates*. PhD Thesis, Universite de Nantes, laboratoire de petrologie et de mineralogie, Nantes, Pp. 351.
- Le Maitre, R.W., 2002. *Igneous Rocks: A classification and glossary of terms*. Cambridge University Press, Cambridge, Pp. 256.
- Olarewaju, V.O., 1988. REE in charnockitic and granitic rocks of Ado-Ekiti – Akure, southwestern Nigeria: In P.O. Oluyide *Precambrian Geology of Nigeria: A publication of Geological Survey of Nigeria*, Pp. 231 – 239.
- Oyawoye, M.O., 1964. The contact relationship of charnockite and granite gneiss at bauchi, Northern Nigeria: *Geological magazine*, 101, Pp. 138 – 144.
- Ozeigbe, E.J., Olarewaju, V.O., Ocan, O.O., Costin, G., 2020. Retrogression of orthopyroxene-bearing gneiss of Iboropa Akoko, southwestern Nigeria. *Materials and Geoenvironment*. <https://doi.org/10.2478/rmzmag.2020-0009>.
- Parras, K., 1958. On the charnockites in the light of a highly metamorphic rock complex in southwestern Finland. *Bullentin Comm Geol. Finlande*, Pp. 181.
- Perchuk, L.L., Gerya, T.W., 1993. Fluid control of charnockitization. *Chemical Geology*, 108, Pp. 175 – 186.
- Pichamuthu, C.S., 1960. Charnockite in the making. *Nature*, 188, Pp. 135 – 136.
- Raase, P., 1974. Al and Ti contents of hornblende, indicators of pressure and temperature of regional metamorphism. *Contributions to Mineralogy and Petrology*, 45 (3), Pp. 231- 236.
- Rahaman, M.A., Ocan, O.O., 1988. The nature of granulite facies metamorphism in Ikare area, southwestern Nigeria. In *Precambrian Geology of Nigeria*, edited by P. Oluyide, Pp. 157 – 163.
- Rajesh, H.M., 2012. A geochemical perspective on charnockite magmatism in Peninsular India. *Geoscience Frontiers*, (6), Pp. 773 – 788.
- Rigby, M.J., Droup, G.T.R., 2011. Fluid- absent melting versus CO₂ streaming during the formation of polytic granulites: A review of insights from cordierite fluid monitors, origin and evolution of Precambrian high grade gneiss terranes with special emphasis on the Limpopo complex of South Africa, 207, Pp. 39.
- Rollinson, H.R., Tarney, J., 2005. Adakites- A key to understanding LILE depletion in granulites. *Lithos*, 79, Pp. 61 – 81.
- Spear, F.S., 1981. An experimental study of hornblende stability and variability in amphibolites. *American Journal of Science*, 281 (6), Pp. 697 – 734.
- Srinakantappa, C., Prakash, C., Narasimha, K.N., 1988. Retrogression of charnockite in Moyar shear zone of Tamil Nadu. *Journal of the Geological Society of India*, 11, Pp. 117 – 124.
- Yang, Q.Y., Santosha, M., Tsunogae, T., 2014. First report of Paleoproterozoic incipient charnockite from the North China Craton: Implications for ultra-high temperature metasomatism. *Precambrian Research*, 243, Pp. 168 – 180.